Supporting Information

MXene-supported NiMn-LDHs as efficient electrocatalysts towards enhanced oxygen evolution reactions

Yi Liu[a,*], Liang Bai[a], Tao Li[a], Haixing Liu[a], Xiaofei Wang[a], Lifeng Zhang[a],

Xiaodong Hao[b,*], Chaozheng He[c] and Shouwu Guo[a,d,*]

[a] *School of Materials Science and Engineering, Shaanxi Key Laboratory of Green Preparation and Functionalization for Inorganic Materials, Institute of Frontier Science and Technology Transfer, Shaanxi University of Science and Technology, Xi'an, 710021, China.*

[b] *Materials Institute of Atomic and Molecular Science, Shaanxi University of Science and Technology, Xi'an, 710021, China.*

[c] *Institute of Environment and Energy Catalysis, Shaanxi Key Laboratory of Optoelectronic Functional Materials and Devices, School of Materials Science and Chemical Engineering, Xi'an Technological University, Xi'an 710021, China.*

[d] *Department of Electronic Engineering, School of Electronic Information and Electrical Engineering, Shanghai Jiao Tong University, Shanghai 200240, China.*

* Corresponding Authors: Yi Liu, E-mail: liuyi@sust.edu.cn

Xiaodong Hao, E-mail: hao.xiaodong@sust.edu.cn

Shouwu Guo, E-mail: swguo@sjtu.edu.cn

Experimental Section

Materials

$NiCl_2 \cdot 6H_2O$, $MnCl_2 \cdot 4H_2O$, and $C_6H_{12}N_4$ were purchased from Tianjin Tianli Chemical Reagent Co., Ltd, Sinopharm Chemical Reagent Co., Ltd (SCRCL), and Tianjin kemio Chemical Reagent Co., Ltd, respectively. Ti_3AlC_2, LiF, and HCl were purchased from Jilin Yiyi Technology Co., Ltd, Shanghai Aladdin Biochemical Technology Co., Ltd, and SCRCL, respectively. All aqueous solutions were prepared utilizing deionized (DI) H_2O. All of the chemicals were analytical grade reagents that had not been purified further.

Materials Characterization

The X-ray diffraction spectra (XRD; D/max-2200 with Cu K_α radiation $\lambda = 1.5418$ Å) was utilized to study the crystal structure of catalysts. The morphology and crystal structure of Ti_3AlC_2 MAX phase, Ti_3C_2 MXene, NiMn-LDHs, and NiMn-LDHs/Ti_3C_2-MXene hybrids were observed by utilizing scanning electron microscopy (SEM; HitachiS-4800). The elemental composition of NiMn-LDHs/Ti_3C_2-MXene hybrids was characterized by utilizing energy dispersive X-ray spectra (EDS, Oxford 6587). The aberration-corrected scanning transmission electron microscopy (Ac-STEM) characterization was conducted by using a JEM-ARM 300F (Cold Field Emission Gun) with both probe and image correctors at the accelerating voltage of 300 kV. The convergence angle was ~ 24.5 mrad, and the collection angle of the high angle annular dark field (HAADF) detector was 54-220 mrad. The energy dispersive X-ray (EDS) spectra were recorded using a Dual-EDS system (JED-2300T) incorporating two large windowless SDD detectors with a total solid angle of 2.2 sr. The surface electronic state and the binding energies of NiMn-LDHs and NiMn-LDHs/Ti_3C_2-MXene hybrids were analyzed by utilizing the X-ray Photoelectron Spectroscopy (XPS; Axis Supra, Al Kα X-ray). All the binding energies were corrected by C 1s line at 284.8 eV as standard. And prior peak deconvolution, all spectra fitting, and background subtraction were completed.

Electrochemical measurements

Autolab (AUT87657) electrochemical workstation was utilized to estimate electrochemical performance of NiMn-LDHs and NiMn-LDHs/Ti_3C_2-MXene hybrids at room temperature (RT, 25 °C). The three electrodes of the OER test system include glassy carbon electrode (GCE, R = 2.5 mm) loaded with catalyst (working electrode), saturated Ag/AgCl electrode (reference electrode) and Pt sheet electrode (counter electrode). The reference electrode has been calibrated before utilization. The working

electrode were prepared as follows: 4 mg catalyst samples were dispersed into mixed aqueous (DI H_2O: 480 μL; C_2H_5OH: 500 μL; Nafion: 20 μL). Subsequently, the mixed aqueous were sonicated for 30 min to get uniformly dispersed ink. Ultimately, 10 mL of ink (catalyst loading: ~ 0.2 mg cm^{-2}) was dropped onto the GCE.

Before the measurement, 1 M KOH solution (500 mL) was saturated with O_2 for 30 minutes. During the test, the O_2 flow was utilized to protect the electrolyte. Besides, electrodes were activated to the stable status via taking 20-30 cycles of cyclic voltammetry (CV) measurement (in the range of 0.1-0.9 V). Simultaneously, the linear sweep voltammetry (LSV) were gained under certain conditions (rotating disc electrode speed: 1600 rpm; scanning speed: 10 mV/s; iR-compensation: 85%). The reversible hydrogen electrode (RHE) was utilized as a reference for all potential calculations: $E_{vs. RHE}$ = $E_{vs. Ag/AgCl}$ + 0.059pH + 0.198V; the overpotential (η) was computed via η (V) = $E_{vs. RHE}$ - 1.23V. The electrochemical impedance spectroscopy (EIS) was obtained at specific conditions (potential vs. RHE: 1.73V; frequency range: 10^{-1} ~ 100 kHz). The CV measurement was utilized to estimate electrochemistry active area (potential vs. RHE range: 0-0.1V; scanning speed range: 5~100 mV/s). The chronopotentiometric measurements were investigated over a 10-hour period (potential vs. RHE: 1.52, 1.58, and 1.56 V for NT-10, NiMn-LDHs, and IrO_2, respectively.).

Computational method

The structural and electronic properties of NiMn-LDHs and NiMn-LDHs/Ti_3C_2-MXene hybrids were computed by utilizing first-principle calculation software VASP. The Perdew-Burke-Ernzerhof (PBE) functional with the Generalized Gradient Approximation (GGA) was utilized for all computing tasks. Meanwhile, the van der Waals force was utilized to correct PBE functional. Here, the Hubbard-U correction was used to describe the localized d-electrons of Ni, Mn and Ti in electrocatalysts.[1] The value of U (3.8 eV for Ni, 3.06 eV for Mn and 2.58 eV for Ti) in this research system can be obtained from the literatures.[2-4] For NiMn-LDHs/Ti_3C_2-MXene hybrids, the (001) surface of NiMn-LDHs was applied to couple with (001) surface of Ti_3C_2 MXene, possessing the smallest lattice mismatch. In the process of structural optimization, all ion position optimization algorithms utilized the conjugate gradient method. During the relaxations, the energy convergence criterion, force convergence criterion, and plane wave cutoff energy were set to 10^{-5} eV, -0.03 eV/Å, and 400 eV, respectively. All structural models were applied with a vacuum layer of 15 Å (direction: z-axis) to avoid the impact of periodic mirroring on itself, the spin-polarized label (ISPIN) was opened in all calculation tasks and the Brillouin zone k-points was chosen as 3×5×1.
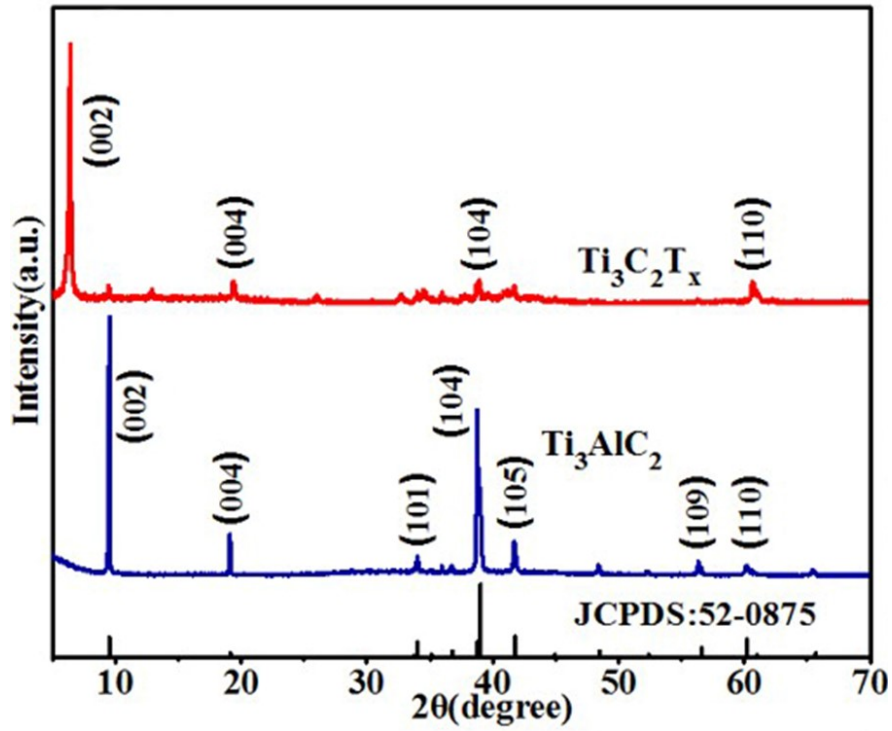
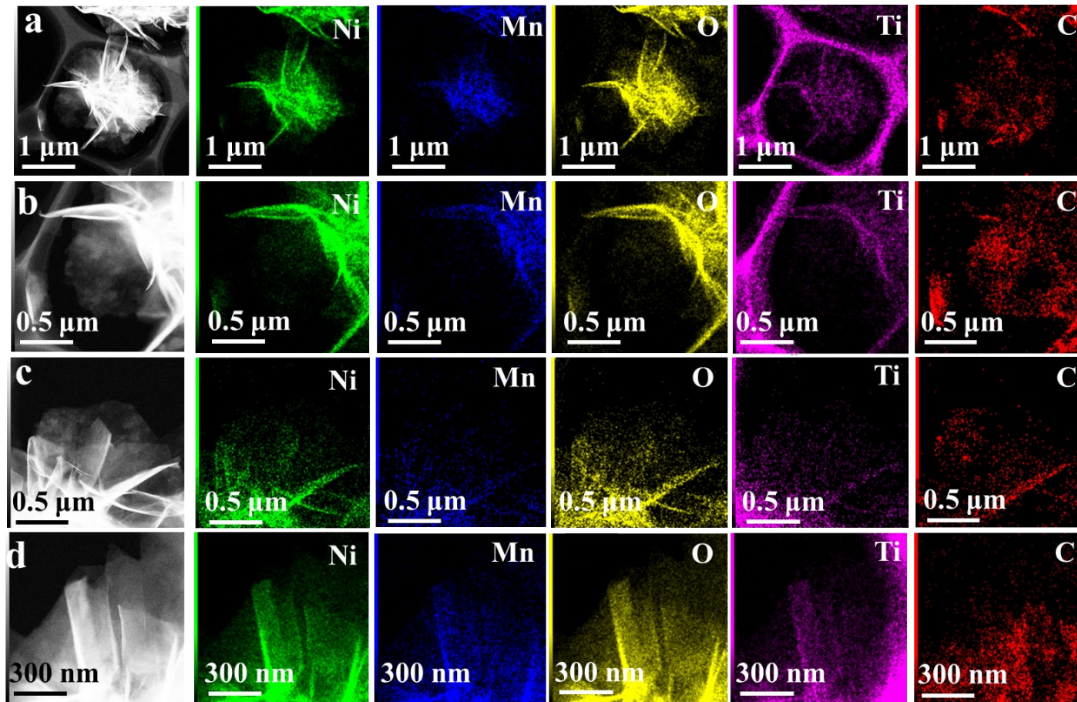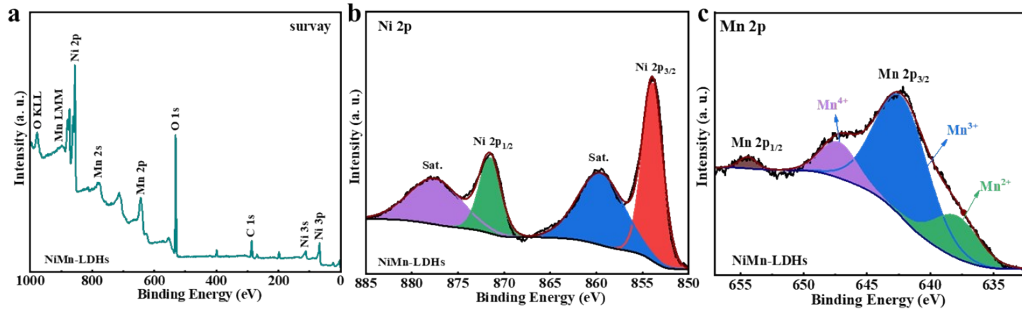**Fig. S1** XRD patterns of Ti_3AlC_2 MAX phase and Ti_3C_2 MXene.
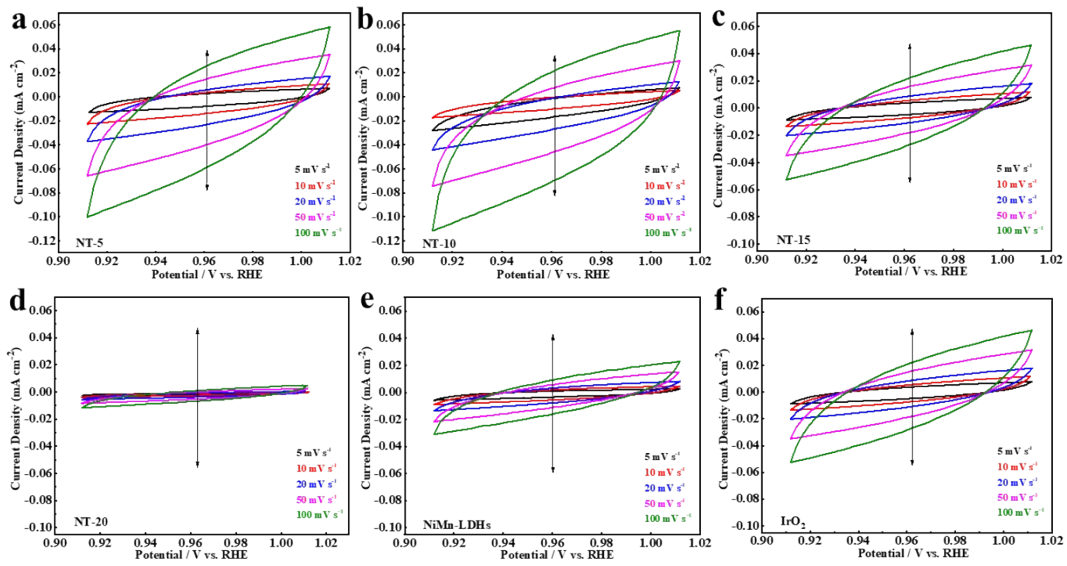

Fig. S2 The elemental EDS mapping of NT-10 with different magnifications: (a-d) ADF images, followed by the individual elemental EDS mapping of Ni, Mn, O, Ti, and C, respectively.

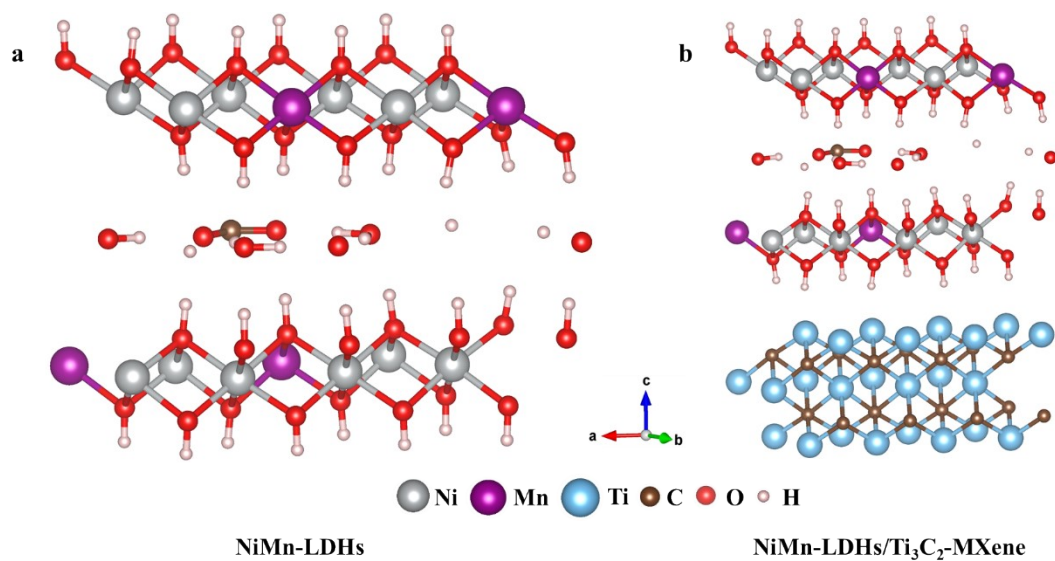**Fig. S3** XPS spectra of the NiMn-LDHs. (a) XPS survey spectrum, (b) Ni 2P, and (c) Mn 2P.

Fig. S4 The electrochemical active surface area characterizations in 1 M KOH. CV cycles at scan rate of 5, 10, 20, 50, and 100 mV s⁻¹ for (a) NT-5, (b) NT-10, (c) NT-15, (d) NT-20, (e) NiMn-LDHs, and (f) IrO₂.
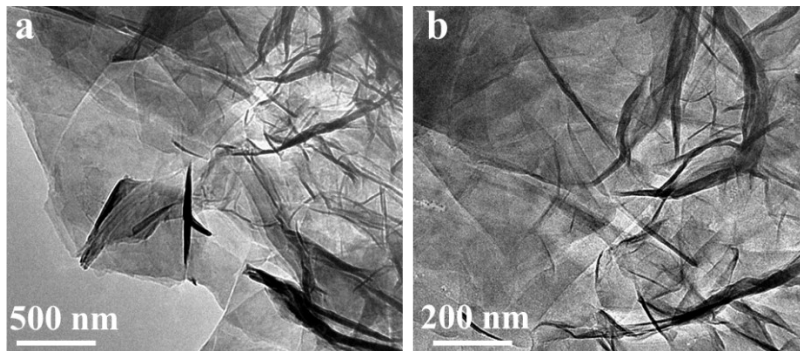
Fig. S5 TEM images of the NT-10 after the stability test: (a) 500 nm; (b) 200 nm.

Fig. S6 The schematic of (a) NiMn-LDHs and (b) NiMn-LDHs/Ti$_3$C$_2$-MXene. The grey, purple, wathet, brown, red and, white spheres represent Ni, Mn, Ti, C, O, and H atoms, respectively.

Table S1. Recent reports on the OER performance of LDHs-based electrocatalysts in 1M KOH.

Electrocatalysts	Electrolytes	Overpotential at 10 mA cm^{-2} (mV)	Tafel slop value (mV dec^{-1})	Ref.
FeNi-LDHs/Ti$_3$C$_2$-MXene	1.0 M KOH	298	43	5
NiCo-LDH	1.0 M KOH	420	113	6
CNT@NiCo-LDH-Ov	1.0 M KOH	318	57	7
Ni$_5$Mn-LDH/MWCNT	1.0 M KOH	350	83.5	8
NiCo-LDH/NA	1.0 M KOH	307	64	9
Exfoliated NiFe-LDHs	1.0 M KOH	300	40	10
CoCo-LDH 2D nanomesh	1.0 M KOH	319	42	11
ZIF-67/CoNiAl-LDH	1.0 M KOH	303	88	12
AE-CoFe-LDH	1.0 M KOH	300	41	13
NiCoFe-LDHs	1.0 M NaOH	288	134	14
NiMn-LDH	**1.0 M KOH**	**356**	**120.6**	**This work**
NiMn-LDHs/T$_3$C$_2$-MXene hybrids	**1.0 M KOH**	**294**	**83.7**	**This work**

3

References

1   S. L. Dudarev, G. A. Botton, S. Y. Savrasov, C. J. Humphreys, A. P. Sutton, Electron-energy-
     loss spectra and the structural stability of nickel oxide: An LSDA+U study. Phys. Rev. B,
     1998, **57**, 1505–1509. https://doi.org/10.1103/physrevb.57.1505.

2   K. Fan, H. Chen, Y. Ji, H. Huang, P. M. Claesson, Q. Daniel, B. Philippe, H. Rensmo, F. Li and
     Y. Luo. Nickel–vanadium monolayer double hydroxide for efficient electrochemical water
     oxidation. Nat. Commun., 2016, **7**, 11981. https://doi.org/10.1038/ncomms11981.

3   Y. Bi, Z. Cai, D. Zhou, Y. Tian, Q. Zhang, Q. Zhang, Y. Kuang, Y. Li, X. Sun and X. Duan.
     Understanding the incorporating effect of Co^{2+}/Co^{3+} in NiFe-layered double hydroxide for
     electrocatalytic oxygen evolution reaction. J. Catal., 2018, **358**, 100-107.
     https://doi.org/10.1016/j.jcat.2017.11.028.

4   M. Luo, Z. Cai, C. Wang, Y. Bi, L. Qian, Y. Hao, L. Li, Y. Kuang, Y. Li, X. Lei, Z. Huo, W.
     Liu, H. Wang, X. Sun and X. Duan. Phosphorus oxoanion-intercalated layered double
     hydroxides for high-performance oxygen evolution. Nano Res., 2017, **10**, 1732-1739.
     https://doi.org/10.1007/s12274-017-1437-2.

5   M. Z. Yu, S. Zhou, Z. Y. Wang, J. J. Zhao and J. S. Qiu. Boosting electrocatalytic oxygen
     evolution by synergistically coupling layered double hydroxide with MXene. Nano Energy,
     2018, **44**, 181-190. https://doi.org/10.1016/j.nanoen.2017.12.003.

6   J. Jiang, A. Zhang, L. Li and L. Ai. Nickel-cobalt layered double hydroxide nanosheets as high-
     performance electrocatalyst for oxygen evolution reaction. J. Power Sources, 2015, **278**, 445-
     451. https://doi.org/10.1016/j.jpowsour.2014.12.085.

7   H. Wang, Y. Yuan, J. L. Gu, Z. C. Jia, Z. S. Lu, Z. Y. Bai, L. Yang and X. L. Yang. Facile one-
     pot synthesis of layered double hydroxides nanosheets with oxygen vacancies grown on carbon
     nanotubes for efficient oxygen evolution reaction. Journal of Power Sources, 2020, **467**,
     228354. https://doi.org/10.1016/j.jpowsour.2020.228354.

8   G. Jia, Y. Hu, Q. Qian, Y. Yao, S. Zhang, Z. Li and Z. Zou. Correction to Formation of
     Hierarchical Structure Composed of (Co/Ni)Mn-LDH Nanosheets on MWCNT Backbones for
     Efficient Electrocatalytic Water Oxidation. ACS Appl. Mater. Interfaces, 2016, **8**, 14527-34.
     https://doi.org/10.1021/acsami.6b09564.

9   C. Yu, Z. Liu, X. Han, H. Huang, C. Zhao, J. Yang and J. Qiu. NiCo-layered double hydroxides
     vertically assembled on carbon fiber papers as binder-free high-active electrocatalysts for water
     oxidation. Carbon, 2016, **110**, 1-7. https://doi.org/10.1016/j.carbon.2016.08.020.

10   F. Song and X. Hu. Exfoliation of layered double hydroxides for enhanced oxygen evolution
     catalysis. Nat. Commun., 2014, **5**, 4477. https://doi.org/10.1038/ncomms5477.

11   M. Qin, S. Li, Y. Zhao, C. Lao, Z. Zhang, L. Liu, F. Fang, H. Wu, B. Jia, Z. Liu, W. Wang, Y.
     Liu and X. Qu. Nanomesh: Unprecedented Synthesis of Holey 2D Layered Double Hydroxide
     Nanomesh for Enhanced Oxygen Evolution. Adv. Energy Mater., 2019, **9**, 1803060.
     https://doi.org/10.1002/aenm.201970003.

12   J. Xu, Y. Zhao, M. Li, G. Fan, L. Yang and F. Li. A strong coupled 2D metal-organic
     framework and ternary layered double hydroxide hierarchical nanocomposite as an excellent
     electrocatalyst for the oxygen evolution reaction. Electrochim. Acta., 2019, **307**, 275-284.
     https://doi.org/10.1016/j.electacta.2019.03.210.

13   P. Zhou, et al. Acid-etched Layered Double Hydroxides with Rich Defects for Enhancing the Oxygen Evolution Reaction. Chem. Commun., 2017, **53**, 11778-11781. https://doi.org/10.1039/C7CC07186H.

14   M. Zhang, Y. Q. Liu, B. Y. Liu, Z. Chen, H. Xu, K. Yan, Trimetallic NiCoFe-Layered Double Hydroxides Nanosheets Efficient for Oxygen Evolution and Highly Selective Oxidation of Biomass-Derived 5-Hydroxymethylfurfural, ACS Catalysis, 2020, **10**, 5179-5189. https://dx.doi.org/10.1021/acscatal.0c00007.